Controlling DNA Translocation through Gate Modulation of Nanopore Wall Surface Charges

Yuhui He,[†] Makusu Tsutsui,[†] Chun Fan,[‡] Masateru Taniguchi,[†,*] and Tomoji Kawai[†,*]

[†]The Institute of Scientific and Industrial Research, Osaka University, 8-1 Mihogaoka, Ibaraki, Osaka 567-0047, Japan, and [‡]Computer Center of Peking University, Beijing 100871, China

ABSTRACT One major challenge of nanopore-based DNA sequencing technology is to find an efficient way to reduce DNA translocation speed so that each nucleotide can reside long enough in the pore for interrogation. Here we report the electrical tuning of DNA translocation speed by gate modulation of nanopore wall surface charges. We find that native surface-charge-induced counterions in the electroosmotic layer substantially enhance advection flow of fluid, which exerts stronger dragging forces on the translocating DNA, and thereby lowering the DNA translocation speed. We propose a feedback device architecture to regulate DNA translocation by modulating the effective wall surface charge density σ_w^* *via* lateral gate voltages—at the beginning, a positive gate bias is applied to weaken σ_w^* in order to enhance the capture rate of DNA molecule; upon detection of ionic current variance indicating DNA has been driven into the nanopore, gate bias is turned to be negative so that σ_w^* is reinforced and DNA translocation is retarded. We show that a gate electric field can dramatically decrease the DNA translocation speed at a rate about 55 μm/s per 1 mV/nm.

KEYWORDS: nanopore sequencing · wall surface charges · gate control

Over the past decades, nanopores and nanochannels have emerged as promising platforms for single-molecule manipulation and detection.[1−4] Among various applications, nanopore-based DNA sequencing technique is currently under intensive study with the prospect of being a label-free single-molecule sequencing technique.[4,5] The original proposal is based on the ionic current blockade mechanism by a volume exclusion effect of a single-moelcule DNA electrophoretically driven through a nanopore that enables identification of the base sequence by measuring the characteristic temporary change of transpore ionic current or transverse tunneling current.[1,2,6−12] A crucial step toward nanopore sequencing is to reduce the DNA translocation speed in the pore so that each nucleotide can remain inside the nanopore long enough to achieve single-base resolution.[4] A straightforward method is to decrease the applied electric driving field. However, such an approach will also cause substantial decreasing of the ionic currents, which will lead to severely deteriorated signal-to-noise ratio (SNR) considering the strong background noise in the aqueous solution environment. Another restriction for lowering driving voltage is the existence of threshold voltage for capturing DNA into the nanopore.[13,14] Thus, a trade-off has to be made between lowering DNA translocation speed and keeping SNR and DNA capture rate when trying to use a smaller electric driving field.

In order to slow down the DNA translocation, several strategies have been proposed, such as tuning viscosity of the solution,[15] the salt concentration,[16] exerting an extra mechanical dragging force by using optical tweezers,[17,18] and using a chemically functionalized nanopore.[12,19] On the other hand, we find that both the ionic currents and DNA translocation speed would be substantially affected by the presence of surface charges on the wall. It enlightens a promising approach for regulating DNA translocation by adjusting the effective wall surface charge density with lateral gate voltages. We thus propose a feedback gate-control device architecture for guiding DNA translocation through a nanopore. By reinforcing effective wall surface charge density σ_w^* *via* negative gate bias ($V_G < 0$), a stronger electroosmotic flow opposite to DNA translocation is induced and it significantly decreases DNA speed inside the nanopore (*retarding stage*). However, such a retarding flow would also block the next DNA molecules from being driven into the pore for continuous high-throughput sequencing. In fact, a positive gate bias ($V_G > 0$) is required to weaken σ_w^* and the corresponding electroosmotic flow in order to enhance the capture rate of DNA by the nanopore (*capture stage*). That is, the retarding stage and capture stage have quite different demands on gate bias. Here, a feedback

* Address correspondence to taniguti@sanken.osaka-u.ac.jp, kawai@sanken.osaka-u.ac.jp.

Received for review March 3, 2011 and accepted June 12, 2011.

Published online June 13, 2011
10.1021/nn201883b

control by ionic current signal is introduced as a solution: by monitoring ionic current changes whether DNA has been driven into a nanopore and is resolved, and this feedback determines that V_G should be <0 at the retarding stage or >0 at the capture stage. Several advantages are expected by utilizing the proposed device setup: it is capable of decreasing the DNA translocation speed while keeping the baseline levels of ionic currents and, hence, SNR unaltered; a real-time and more precise tuning of DNA translocation can be achieved by adjusting the amplitude of gate voltage, thus providing more flexibility; also, a gate-bias controlling approach is compatible with the conventional semiconductor industry, promising the integration and mass production.[20,21]

THEORY

Figure 1 gives a schematic view of the system under investigation: the nanopore is approximated with a cylinder, and the uncoiled DNA inside the nanopore is modeled as a cylinder with radius a locating in the center of the nanopore. Figure 1b,c describes situations without and with wall surface charges. Without the charges, only one electrical double layer (EDL) is formed near the surface of DNA; with the charges, another EDL is formed near the surface of the pore wall. A series of equations are employed to describe the potential and ionic concentration distributions, fluid flow, ionic transport, and DNA translocation in the nanopore:

(1) Poisson−Boltzmann equation for the ionic charge distribution in the liquid inside the nanopore:

$$\nabla^2\Phi = -\frac{\rho_e}{\varepsilon_f} = -\frac{e\sum_i z_i n_i}{\varepsilon_f} \quad (1)$$

$$n_i = n_i^0 \exp\left(-\frac{ez_i\Phi}{k_B T}\right) \quad (2)$$

In the above equation, Φ is the electrical potential, ρ_e is the net charge density, ε_f is permittivity of the fluid, n_i is the concentration of the ith ionic species, n_i^0 is far-field concentration of that species, and z_i is the valency. For KCl solution, the equation is simplified as $\nabla^2\bar{\Phi} = (\sinh\bar{\Phi})/(\lambda_D^2)$, where $\bar{\Phi} = (e\Phi)/(k_B T)$, $\lambda_D = ((\varepsilon_f k_B T)/(2N_{KCl}e^2))^{1/2}$ is the Debye length, and $N_{KCl} = n_K^0 = n_{Cl}^0$ is the salt concentration of KCl. As seen in Figure 1 and Figure 2, λ_D characterizes the thickness of EDL formed near the surfaces of DNA and charged pore wall.

(2) Navier−Stokes equation for the fluid motion:

$$\rho\left(\frac{\partial\vec{v}}{\partial t} + \vec{v}\cdot\nabla\vec{v}\right) = -\nabla p + \mu\nabla^2\vec{v} + \vec{f} \quad (3)$$

$\vec{v}$ is the velocity of the liquid, p is the hydrostatic pressure, μ is the fluid viscosity, and f is the density of external forces on the liquid. At steady state, it is

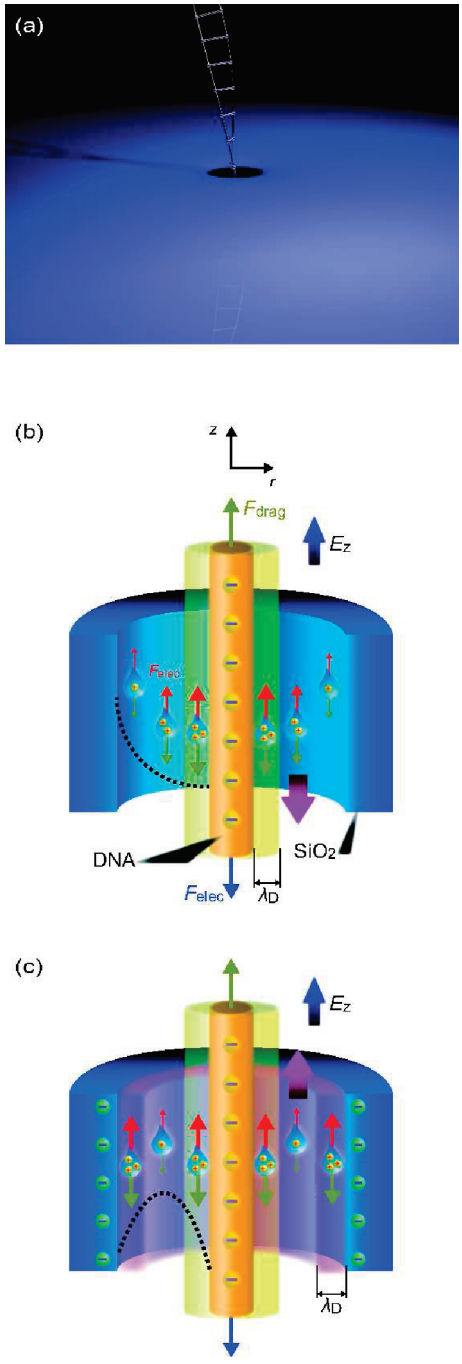

Figure 1. Schematic illustrations depicting a nanopore system used to investigate DNA translocation through a solid-state nanopore. (a) Double-stranded DNA passing through a solid-state nanopore. (b) Nanopore without wall surface charges. The DNA is modeled as a cylinder locating at the center of the nanopore, with homogeneous charge distribution along the *z*-axis. The closer the water drops to the DNA surface, the larger counterion concentration inside, thus the stronger the electrical driving forces F_{elec} along E_z. (c) Nanopore with surface charges on the pore inner wall: two electrical double layers (EDL) form at the DNA surface and at the wall surface. The dashed lines in (b) and (c) depict the *z*-component liquid velocity v_a. Blue arrows represent the electric driving force on negatively charged DNA, red arrows represent that on counterions in EDL, and dark yellow arrows represent hydrodynamic dragging forces on liquid drops and on DNA. In addition, directions of advection flows in the nanopore are characterized with purple arrows.

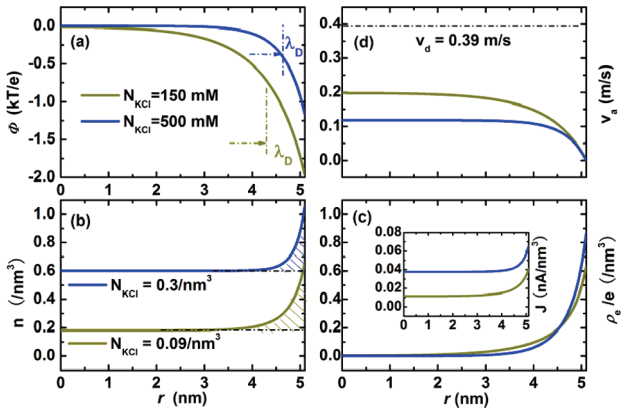

Figure 2. Distribution of electrical potential Φ (a), ionic concentration *n* (b), ionic charge concentration ρ_e/e (c), advection velocity of ions in the fluid v_a (d), and ionic current density *J* (inset in (c)) along the nanopore radius *r* when there is no DNA inside. Here the parameters are set as those in the experiments:[25] radius of the nanopore *R* = 5.1 nm, dark yellow line is for N_{KCl} = 150 mM = 0.09/nm^3, and blue line N_{KCl} = 500 mM = 0.3/nm^3. The applied electrical field, E_z = 5.05 mv/nm, and the surface charge density of the nanopore inner wall, $\sigma_w = -49$ mC/m^2, are the optimal data fit with the open-pore currents observed in the experiments. The associated Debye lengths are characterized in (a), the electrical double layers formed near the nanopore inner wall are marked with oblique lines in (b), the ionic drift velocity is marked with dash-dot line in (d), and for the convenience of comparing drift current and advection current, ρ_e/e is plotted in (c) instead of ρ_e.

appropriate to write the equation as $\mu\nabla^2 v_a = 2n_0 eE_z \sinh \vec{\phi}$ since the Reynolds number of fluid in the nanopore is quite small.[16] Here v_a is the *z*-component of the liquid velocity $\vec{v}$, and E_z is applied electric field.

(3) DNA motion in the liquid inside the nanopore: For a small DNA segment with length *dl*, the forces exerted are the sum of driving force dF_{elec} by the electrical field, and dragging force dF_{drag} from the fluid environment:

$$dF_z = E_z\lambda_{DNA}dl + \mu\frac{\partial v_a}{\partial r}|_{r=a}2\pi a dl + 6\pi\mu R_g\frac{dR_g}{dt}\frac{dl}{\alpha L_{DNA}} \quad (4)$$

where R_g is the gyration radius of untranslocated parts of the polymer within the *cis* chamber.[22,23] The second term denotes viscous force by liquid within the nanopore, while the third term does that by liquid at the entrance of the nanopore.[24] Here $6\pi\mu R_g(dR_g)/(dt)$ is the Stokes force on the awaiting-to-translocate DNA residues, L_{DNA} is contour length of the polymer and a parameter α is introduced to denote the ratio transmitted to those being translocating within nanopore.

(4) Nernst−Plank equation for ion motion in the liquid:

$$\frac{\partial n_i}{\partial t} = -\nabla\cdot\vec{N}_i = -\nabla\cdot(n_i\vec{v} - D_i\nabla n_i - \mu_i n_i\nabla\Phi) \quad (5)$$

$\vec{N}_i$ is the ionic flux density of the *i*th ionic species, D_i is the diffusivity, and μ_i is the mobility.

Semiempirical Evaluation of Wall Surface Charge Density. We deduced a wall surface charge density from the open-pore ionic currents reported in experiments,[25] where the diameter and length of SiO_2 nanopores are about 10 and 20 nm, respectively. The drift current formula $I_d = e(\mu_K n_K + \mu_{Cl} n_{Cl})E_z\pi R^2 \doteq 2\pi R^2 N_{KCl} e\mu_K E_z$ gives a rough estimation of the ionic current, where I_d is the drift current, $\mu_{K(Cl)}$ is the mobility of K(Cl) ions, $n_{K(Cl)}$ is K(Cl) ion density, E_z is the electric driving field along the *z* direction, *R* is nanopore radius, and N_{KCl} is salt concentration. However, we find that the experimentally observed current values do not comply with such a naive estimation: experimentally, *I* = 1.36 nA when N_{KCl} = 150 mM, indicating that *I* should be 4.53 nA when N_{KCl} = 500 mM, while the observed ionic current is 3.36 nA, obviously smaller than the expected value. Qualitatively, this can be attributed to the existence of electroosmotic flow near the charged nanopore wall. The Debye length λ_D is smaller at higher salt concentration, and the electrical potential drop ΔΦ also becomes smaller within λ_D. This is demonstrated in Figure 2a, where distribution of Φ along the nanopore radius is plotted. Consequently, the ionic concentration *n* within EDL could not keep the same ratio as in the interior region as seen in Figure 2a,b. Further investigation shows that by setting the wall surface charge density of $\sigma_w = -49$ mC/m^2 and the applied electrical field of E_z = 5.05 mV/nm, the calculated ionic currents are in accordance with the experimental data. We stress that the inferred value of pore surface charge density is typical for SiO_2 surfaces,[26,27] and the estimated E_z is also quite consistent with the experiments—where a voltage of 120 mV was applied to the 20 nm thick nanopore during the DNA translocation.

Figure 2d plots the distribution of the fluid velocity v_a along the nanopore radius with the wall surface charge of $\sigma_w = -49$ mC/m^2. It demonstrates that the lower the salt concentration N_{KCl}, the larger the liquid velocity. Physically, this behavior is caused by the stronger electrical driving forces F_{elec} due to the larger space expansion of the net ionic charges ρ_e at smaller salt concentration, as seen in Figure 2c. Besides, we should keep in mind that the liquid velocity is, meanwhile,

the advection velocity of ions. Figure 2d suggests that, although the ionic advection velocity v_a is smaller compared to the ionic drift velocity v_d (marked with dash-dot line), they are of the same order. So, it is interesting to see whether the advection current takes an important part in the total ionic current. The following formula indicates that whether the advection current is comparable to the drift current now relies on the proportion of net ionic charge concentration ρ_e over the ionic concentration n.

$$J_a = \rho_e v_a = e(n_K - n_{Cl})v_a \quad (6)$$

$$J_d \doteq (n_K + n_{Cl})e\mu_K E_z \quad (7)$$

By comparing panels b and c in Figure 2, we conclude that the advection current is negligible in the current case due to the much smaller net ionic charge concentration ρ_e. However, we predict that the advection current I_a would play a more important role when the fabricated nanopores have even smaller radius so that the Debye lengths become comparable to the pore dimension. For example, according to our calculation, the measured open-pore ionic current in a R = 3 nm nanopore with salt concentration N_{KCl} = 100 mM (λ_D = 0.96 nm) would be 139% larger than estimated using bulky drift current formula, and 15% of the total ionic current is caused by advection. Such modulation of ionic transport by surface-charge-induced EOF has been discussed in the experiments,[25,27] and it is generalized to the tuning of DNA transport as to be shown in this work.

Now we turn to estimation of ionic currents with DNA translocating in the nanopore. Previous studies have suggested that the effective DNA line charge density λ_{DNA} inside the solution is reduced 50−76% from the bare charge density λ_{bare}.[16,18,25,28] By setting $\lambda_{DNA} = 0.50\lambda_{bare}$, the calculated relative ionic current changes $\Delta I/I_{open}$ and its dependence on the salt concentration N_{KCl} shows excellent agreement with the experiments,[25] as plotted in Figure 3. The reduction of DNA line charge density is ascribed to counterion condensation as predicted by Manning[29] and has been verified by recent experiments.[18,28]

Besides, Figure 3 coincides with the experimental observations that the ionic currents may increase or decrease during DNA translocation depending on the salt concentration.[25,30] The origin of this dramatic change can be found in the inset of Figure 3. The volume exclusion of ions due to the presence of DNA inside the nanopore is characterized by negative oblique lines in the shadow area, while the extra counterions caused by the formation of EDL near the DNA surface is characterized by positive oblique lines. The former effect blocks ions which would contribute to the conductance in the open pore, while the latter raises the number of ions available for the conductance. A balance between these two counteracting effects determines a sign of the ionic current blockade effects.

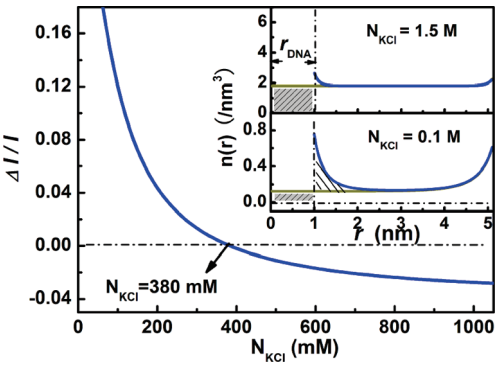

Figure 3. Relative ionic current changes due to DNA translocation in the nanopore as a function of salt concentration N_{KCl}. Here, the DNA cylinder radius a = 1 nm and other parameters are set the same as in Figure 2. The curve matches very well with the experiments[25] when the effective line charge density of DNA is half the bare value: $\lambda_{DNA} = 0.5\lambda_{bare} = -0.48 \times 10^{-9}$ C/m. The inset plots the variation of ionic concentrations n along the nanopore radius when N_{KCl} = 0.1 M and when N_{KCl} = 1.5 M, where the blue curves plot that with DNA inside and the dark yellow curves for the open-pore case.

We further verify the validity of the obtained values of wall surface charge density σ_w and effective line charge density of DNA λ_{DNA} by comparing to other experiments with different SiO_2 nanopore radii and salt concentrations, such as found in some recent work.[28,31] We find that the calculated ionic conductance matches very well with the experiments in which smaller diameter nanopores are used ($R \leq 8$ nm), while they are not so consistent with those experiments where the nanopores are relatively larger ($R \geq 20$ nm). We believe that, for the latter cases, DNA molecules are easily twisted and would pass through the nanopore in a more tangled manner,[32] thus the centrally located cylinder model no longer works for DNA translocation. Fortunately, smaller radius nanopores are much more concern for researchers since more regulated DNA translocation is required for the sequencing purpose.

Surface-Charge-Affected DNA Translocation. We now move on to the tuning of DNA translocation by the presence of σ_w. Figure 4 plots the DNA translocation speed v_z as a function of salt concentration N_{KCl} and nanopore radius R without wall surface charges (Figure 4a) and with the charges (Figure 4b). These plots give a striking view of how substantially the existence of wall surface charges could affect the translocation behavior of DNA. First and most of all, the presence of wall surface charges causes a significant decrease of DNA translocation speed, from hundreds of mm/s to tens of mm/s. In addition, the variance of v_z with N_{KCl} and R becomes quite different when considering the influence by wall surface charges.

Regarding the experiments, the observed DNA translocation speeds are estimated as v_z = 16.5 μm/1.4 ms = 11.8 mm/s and v_z = 16.5 μm/1.2 ms = 13.8 mm/s when N_{KCl} = 150 and 500 mM.[25] They match very well

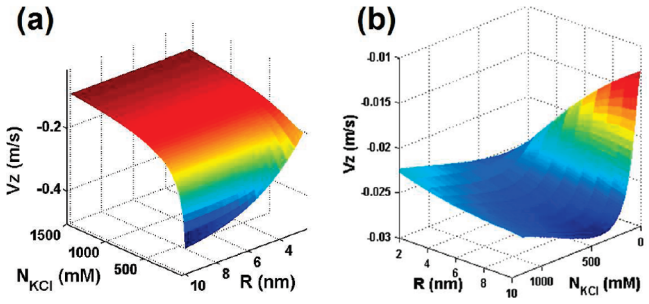

Figure 4. DNA translocation speed v_z as a function of nanopore size R and salt concentration N_{KCl}, without nanopore surface charge (a) and with the pore surface charge density σ_w (b) as in Figure 3.

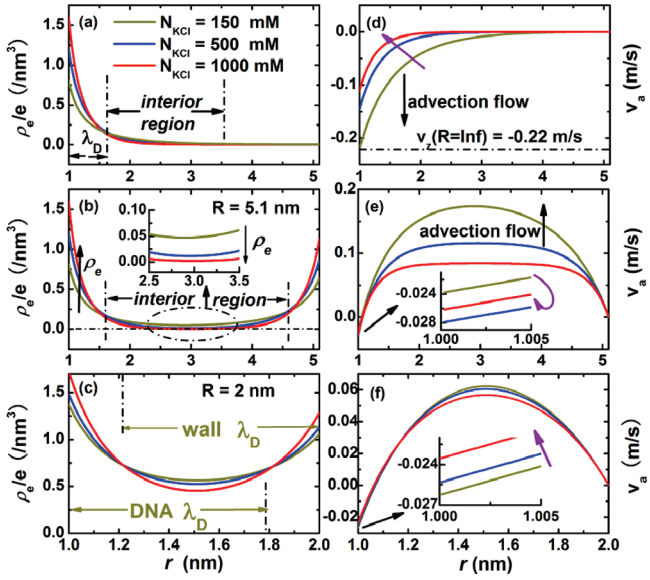

Figure 5. (a) Distribution of ionic charge density ρ_e/e and fluid velocity v_a along the nanopore radius r for various ionic concentration (dark yellow line, N_{KCl} = 150 mM; blue line, N_{KCl} = 500 mM; red line, N_{KCl} = 1000 mM) when the wall surface charge density $\sigma_w = 0$ (a,d) and -49 mC/m^2 (b,e). In addition, an extreme case with pore diameter $R = 2$ nm is plotted in (c) and (f). The dash-dot line in (d) marks the idealized DNA translocation speed in an infinite large nanopore under $E_z = 5.05$ mV/nm and N_{KCl} = 150 mM. Insets in (e) and (f) give amplified views of fluid velocity very near the DNA surface. Here we recall that the fluid velocity at $r = 1$ nm is in fact the DNA translocation speed since a no-slip condition has been assumed. Besides, the variation tendencies of DNA speed with increasing N_{KCl} are marked with violet arrows in the figures.

with our calculated results of 11.9 and 14.0 mm/s separately (the average velocities are half the values shown in the inset of Figure 5e).

To elucidate the origin of DNA translocating speed reduction by wall surface charges shown in Figure 4, we calculate the distribution of ionic charge concentration ρ_e and the fluid velocity v_a along the nanopore radius r (Figure 5). It is anticipated that the larger the ionic charge concentration in the solution, the stronger the electrical driving forces exerted on the liquid, and thus the larger the dragging forces transferred by the liquid to the DNA inside the nanopore, which leads to a decreased DNA translocation speed v_z:

$$\rho_e\uparrow \Rightarrow f_{elec}\uparrow \Rightarrow f_{drag}\uparrow \Rightarrow v_z \rightarrow 0 \qquad (8)$$

This general rule gives a direct answer why DNA translocation speed is significantly reduced by the presence of surface charges on the pore wall: by comparing liquid velocities in Figure 5a,b, we can see that an additional EDL is induced by the wall surface charges, and the advection flow is greatly enhanced along the electric field E_z because of the positive net charges ρ_e in this EDL; thus, as a result, the stronger advection flow now puts stronger dragging force on DNA and substantially retards its translocation.

Nevertheless, several complexities need to be addressed for the variation tendency of v_z with R and N_{KCl} observed in Figure 4:

(1) Without wall surface charges, the larger the salt concentration N_{KCl}, the stronger the ionic charge concentration ρ_e induced in the EDL near DNA surface, as seen in Figure 5a; that is, when $\sigma_w = 0$, $N_{KCl}\uparrow \Rightarrow \rho_e\uparrow$. Thereby, DNA translocation velocity v_z should be decreased, and this is in accordance with the trend shown in Figure 5d, where the purple arrow indicates variation tendency of v_z with increasing N_{KCl}.

(2) The presence of another EDL at the wall surface makes a U-shape turning of ρ_e with increasing N_{KCl},

rather than the monotone increasing behavior when $\sigma_w = 0$. This U-shape turning of ρ_e results in the first increasing and then decreasing DNA translocation speed v_z as N_{KCl} keeps increasing (from dark yellow line to blue line and to red line in Figure 5e). Here the key issue is why ionic charge concentration ρ_e at the beginning decreases with increasing N_{KCl}. The answer is that the interaction between two EDL, one near the DNA surface and the other near the pore surface, leads to much larger ρ_e in the interior region, and when N_{KCl} increases, ρ_e decreases substantially in this region, which overwhelms the increasing of ρ_e in the λ_D region. Figure 5b and the inset clearly demonstrates this ρ_e decreasing when N_{KCl} increases from 150 to 500 mM (from dark yellow line to blue line).

(3) In extremely small nanopores, the two EDL would strongly overlap with each other, as seen in Figure 5c. Accordingly, no interior region exists and the dragging force on DNA is barely determined by $\rho_e(\lambda_D)$. Consequently, the DNA speed is substantially reduced and shows monotonic decreasing with the increasing salt concentration N_{KCl}, as seen in Figure 5f.

At the end of the section, we would like to give some discussion on the Al_2O_3 nanopore, another frequently employed material in the experiments.[33] Our simulation estimates that the pore surface charge density σ_w should be about $+50$ mC/m^2, under which the open-pore currents calculated by our model match very well with those observed in the experiments.[34,35] However, we note that the Al_2O_3 nanopore is *positively* charged, which is opposite to the case of SiO_2. From the viewpoint of electrostatics, a negatively charged DNA molecule could not stay at the center of a positively charged nanopore since it is a potential maximum point. In other words, a small perturbation will cause the translocating polynucleotides to be driven to one corner of the nanopore where van der Waals interaction may dominate the translocation behavior (a detailed investigation is provided in the Supporting Information). Therefore, investigation of DNA movements in the Al_2O_3 nanopore requires theoretical studies resolving microscopic details such as molecular dynamics simulation, which is beyond the scope of this work.

Gate Regulation. Recently, the successful fabrication of gate-all-around nanopores and nanochannels provides an efficient way of manipulating the ionic transport by gate voltages.[20,21] It has been observed that when a negative bias is added to the gate electrodes the ionic current is increased, and such an increase is ascribed to the intensification of surface charge density σ_w on the channel wall, which gives rise to stronger ionic density in the EDL.[20] From previous discussion, we are aware that the tuning of σ_w could also affect the DNA translocation in the nanofluid channels. Here we give a quantitative study on the possible regulation of DNA translocation by gate voltages.

With lateral gate bias, the boundary condition for the Poisson equation should be rewritten as $\Phi'(R) = (\sigma_w + \varepsilon_p E_p)/\varepsilon_f$, where E_p is the electric field generated by lateral gate voltages at the wall surface of the nanopore, in the SiO_2 side, and ε_p is the permittivity of the SiO_2 wall. In the DNA translocation experiments reported so far, no lateral gate voltage has been applied, thus $E_p = 0$ in previous calculations. However, now with the gate bias, the effective surface charge density σ_w^* can be defined as

$$\sigma_w^* = \sigma_w + \varepsilon_p E_p \tag{9}$$

The above equation indicates that a positive gate bias ($V_G > 0$) could weaken σ_w^* while a negative voltage ($V_G < 0$) would enhance it (remember that $\sigma_w < 0$). Considering the strong dependence of DNA speed on σ_w^*, a regulation of DNA translocation by tuning σ_w^* *via* gate voltage now appears on the horizon. Here we propose a feedback gate-control device architecture for the purpose of manipulating DNA translocation through the nanopore. Figure 6 gives a schematic illustration of the device setup: at the beginning, a positive gate voltage is applied to lower the effective surface charge density σ_w^* on the pore wall. As a result, the electroosmotic flow which blocks DNA from entering nanopore is attenuated and thus the capture rate of the DNA molecule is promoted (capture stage). Then, detection of a trans-pore ionic current variation indicates that DNA has been driven into the nanopore. This ionic current change serves as a feedback signal for gate control which triggers a switch of gate voltage to be negative, resulting in reinforced σ_w^* and retarded DNA translocation (retarding stage). The gate bias value to minimize the DNA speed will be investigated in the follow-up. Finally, restoration of ionic current to the open-pore value marks the finish of DNA translocation, and this signal triggers a switch-back of gate voltage to the initial positive value, awaiting another DNA capture and translocation event (reset to capture stage). Here it is worth mentioning that feedback control of DNA translocation through the nanopore is now experimentally feasible because it has been realized on electrical driving voltages.[36] The responding time-scale of the gate-regulated nanopore is estimated as $\tau = RC$, where C is the capacitance of the nanopore and R is the input resistance; τ is less than 1 fs, extremely small since the gate capacitance per unit length $C/L = 2\pi\varepsilon\ln(R/R_{pore})$ is about 1.36×10^{-9} Fm^{-1}.[20]

Before moving onto a quantitative study of gate-tuning DNA translocation during the retarding stage, we indicate that a comprehensive study of optimizing DNA capture rate at the capture stage is beyond the scope of this work. Nonetheless, we would like to give some insight on that topic from the perspective of gate-tuning wall surface charges. In principle, σ_w^* could become positive as long as the gate bias is sufficiently

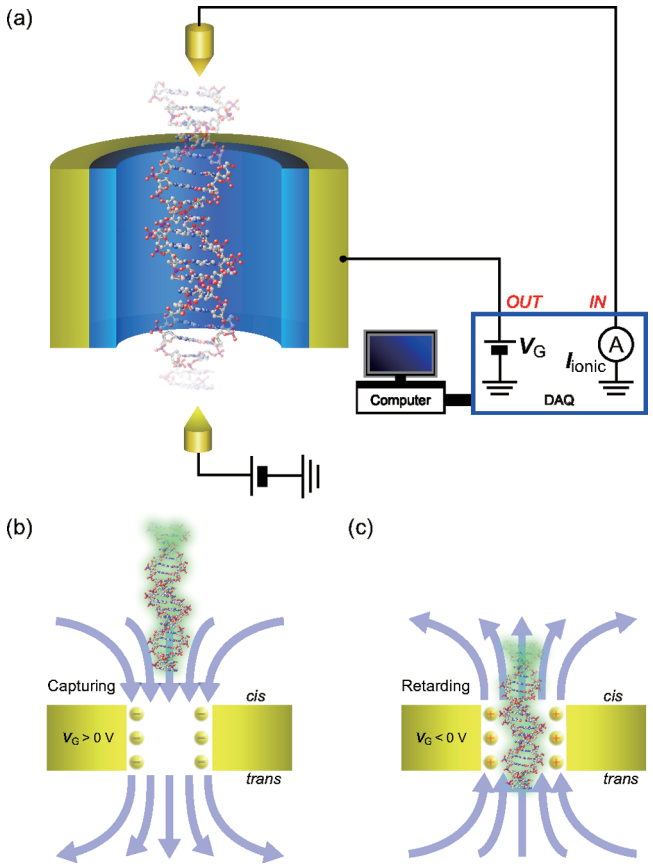

Figure 6. (a) Schematic illustration of gate regulation of DNA translocation *via* feedback of ionic current signal. (b) Capture stage: when the target DNA molecule is swimming in the *cis* chamber, a positive gate voltage V_G is applied to decrease the effective wall surface charge density σ_w^* so that σ_w^*-induced advection flow is attenuated, easing the capture of DNA by a nanopore. A highly idealized case is demonstrated in the figure where σ_w^* turns positive at very large V_G so that σ_w^*-induced electroosmotic flow is now reversed to the same direction as DNA translocation. (c) Retarding stage: once DNA has been driven into the pore, the variation of trans-membrane ionic current triggers a switch of gate bias to a negative value, enhancing σ_w^* and minimizing DNA speed in the pore. Reset to capture stage: upon detection of ionic current restoring to open-pore level, indicating DNA has fully moved into *trans* chamber, gate bias is switched back to the initial positive value, awaiting another capture and translocation event.

large (see red arrow in Figure 7a). Consequently σ_w^*-induced electroosmotic flow is now oriented in the *same* direction as DNA translocation, resulting in an absorbing region around the nanopore.[22,23] Not only will this absorbing region enhance the capture rate of DNA but the velocity gradient in this region will also cause a coil stretch of DNA, another favorable effect for sequencing purposes.[35] A quantitative study on the impact of σ_w^* on threshold voltage for DNA capture is presented in the Supporting Information.

Figure 7a plots DNA translocation speed v_z as a function of effective surface charge density σ_w^*, under various salt concentrations N_{KCl}. On the top axis, the corresponding E_p to σ_w^* values are shown to give a direct view of gate electrical field magnitude. This figure reveals that the DNA translocation speed v_z keeps decreasing as the negative charge density σ_w^* on the wall gets stronger, while the smaller N_{KCl}, the faster the decreasing. From the experiment point of view, it indicates that a negative gate bias will cause a decreasing of DNA translocation speed at rate about 55 μm/s per 1 mV/nm, and by using smaller salt concentration, a smaller gate electric field can be competent to achieve the minimized DNA velocity. Here the speed minimization is defined as $v_z \leq 1$ nm/ms since the two major approaches to nanopore-based DNA sequencing, one by measuring ionic current blockages and the other by measuring transverse tunnel currents or capacitance, require that each nucleotide on the translocating DNA should dwell in the electrical "read" region for more than ~1 ms,[4,37] and the "read" region should be about the size of an individual nucleotide separation of ~0.34 nm.

From Figure 7a, we also note that the DNA speed will finally turn positive if the gate-induced σ_w^* becomes too strong. Such a turning of DNA moving direction is also reported in other theoretical studies.[38] It indicates that experimentally, after detecting the signal of DNA capture, a deliberate tuning of gate voltage V_G should be performed. As DNA movement enters the low speed region marked by the dashed circle in Figure 7a, a small deviation of V_G will induce

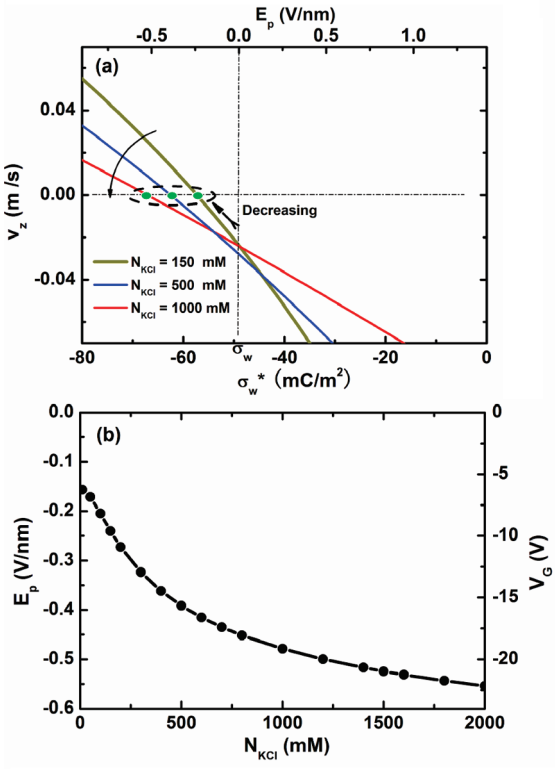

Figure 7. (a) Gate tuning of the DNA translocation velocity. DNA translocating speed v_z as a function of effective wall surface charge density σ_w^* under various salt concentration (dark yellow line, N_{KCl} = 150 mM; blue line, N_{KCl} = 500 mM; red line, N_{KCl} = 1000 mM). The corresponding radial electrical field E_p in SiO_2 is demonstrated on the top axis of the plot. Here the parameters are the same as in Figure 3. The dashed circle characterizes the low speed region of DNA translocation, and those green points mark the critical values of σ_w^* beyond which DNA motion would get reversed. (b) Required E_p to minimize DNA translocating speed as a function of salt concentration N_{KCl}. The corresponding gate bias V_G is plotted on the right axis assuming that the thickness of SiO_2 is about 40 nm.

more negative surface charges on the wall than the intended amount, leading to too strong EOF and thus excessive dragging force on the translocating DNA. As a result, the molecule would withdraw from the nanopore even after being captured into the nanopore mouth. So, it is really challenging to determine the exact amount of intended gate voltage—it should be sufficiently large to induce the required EOF to minimize DNA translocation speed within nanopore; meanwhile, it should not go beyond a critical value to avoid pushing the molecule back to the *cis* chamber. Here the critical values under various salt concentrations are identified by the intersection points in Figure 7a. Our modeling and calculation presented in this work are aimed at that goal: first by measuring open-pore currents under various driving voltages or salt concentrations, the nanopore parameters are extracted based on our model; then the gate-regulated DNA translocation speed curve as Figure 7a is calculated; finally, the exact value of required V_G is found from the obtained curves.

Since salt concentration N_{KCl} is an experimentally tunable parameter for the regulating of required gate electric field E_p to minimize DNA velocity, we further plots the required E_p as a function of N_{KCl} in Figure 7b. The corresponding gate bias V_G is displayed on the right axis assuming a thickness of SiO_2 of ~40 nm.[20] Figure 7b demonstrates that smaller N_{KCl} will facilitate the employment of a smaller E_p and associated V_G for minimizing DNA translocation speed. Here the physical mechanism is that the pore surface-charge-induced EDL will get thicker with decreasing N_{KCl} and thus retard the DNA translocation more substantially because Debye length is larger under smaller N_{KCl}. In contrast, the two EDL, one near DNA surface and other near pore surface, will become thinner and farther from each other under larger N_{KCl}, as seen in Figure 5b. As a result, the retarding force exerted on DNA gets smaller and consequently the decreasing of v_z is slower under larger N_{KCl}, as indicated by the arrow in Figure 7a. However, the required E_p will finally get saturated under very large N_{KCl}, as shown in Figure 7b, due to the saturated distance increasing between two EDL since $\lambda_D \sim N_{KCl}^{-1/2}$.

From the experimental view, the required E_p is very high, in fact, almost reaching the threshold of break down electric field of SiO_2 prepared by chemical vapor deposition (CVD), and using smaller salt concentration may help alleviate such a stringent demand, as illustrated in Figure 7b. However, it should be recalled that a smaller N_{KCl} would result in decreased ionic current and aggravated SNR, and DNA speed gets more sensitive to the change of E_p, as seen in Figure 7a. So in the real experiments, there should be an optimized N_{KCl} to trade off requirements of smaller E_p and better SNR. Here we would like to mention that, although in the current case the required gate electric field E_p is somewhat quite high for the purpose of slowing DNA translocation speed, nonetheless, we can expect that a much smaller E_p is competent since in the experiments, high-κ dielectric material has been used to fabricate nanopores and nanochannels.[20,21]

CONCLUSION

In summary, we have theoretically studied the influence of wall surface charges on the DNA translocation. By comparing the experiments, the quantity of the wall surface charge density and line charge density of DNA segments inside the nanopore have been obtained. We have found that the existence of wall surface charges would substantially reduce the DNA translocation speed by inducing another electroosmotic layer near the wall surface and thus enhancing the advection flow in the nanopore, which puts stronger retarding force on the DNA. Besides, our quantitative study has shown that such a reduction of DNA translocation speed strongly depends on nanopore size and salt concentration since the former characterizes

the *distance* the retarding force induced by wall surface charges has to transmit to DNA while the latter characterizes the *media* for the transmitting. On the basis of the analysis, we have proposed a feedback device architecture for the regulation of DNA translocation speed by tuning effective wall surface densities with gate electrical fields. Our results can provide a guideline for the experimental gate manipulation of DNA passing through a solid-state nanopore.

METHOD

For the Poisson−Boltzmann equations, we have assumed that most of the longitudinal voltage drops within the nanopore, which has been verified by comparing to the experiments.[16,25] Besides there are two Neuman boundary conditions: one at the surface of DNA $\Phi'(r)|_{r=a} = -E_r(a) = -(\lambda_{DNA})/(2\pi a\varepsilon_f)$ and the other at the inner wall surface of nanopore $\Phi'(r)|_{r=R} = -E_r(R) = \sigma_w/\varepsilon_f$. Here E_r is the electrical field along the nanopore radius, λ_{DNA} is the line charge density of DNA segments inside the nanopore, R is the pore radius, and σ_w is surface charge density at the SiO_2 pore wall.

For the Navier−Stokes equations, there are two no-slip boundary conditions at the surface of DNA $v_a|_{r=a} = v_{DNA}$ and at the nanopore wall $v_a|_{r=R} = 0$.

The equation of DNA force is analyzed as follows: the dragging force f_{mouth} by untranslocated DNA segments at the nanopore mouth (third term in eq 4) keeps decreasing as the awaiting-to-pass segments of the polymer become less and less ($R_g \rightarrow 0$); thus, as a first-order approximation, we first neglect it so that DNA translocation can be treated as constant speed movement $dF_z = E_z\lambda_{DNA}dl + \mu(\partial v_a)/(\partial r)|_{r=a}2\pi a dl = 0$,[16] and in this way, we obtain a Neumann boundary condition for the Navier−Stokes equation; then, v^c_{DNA} is calculated with this constant speed model; finally, the average translocation velocity $_{DNA}$ is estimated as half of v^c_{DNA}. A more rigorous treatment is provided in the Supporting Information.

The ionic current is determined by the z-component of $\vec{N}$ shown in eq 3:

$$I = \int_a^R rdr \int_0^{2\pi} d\theta \sum_i ez_i(n_i v_a + n_i\mu_i E_z) \qquad (10)$$

In the above equation, the first term characterizes the advection current $J^i_a = n_i v_a$ of the ith ions while the second term is the drift current $J^i_d = n_i\mu_i E_z$. Here v_a is the ionic advection velocity along the z direction, that is, the z-component of $\vec{v}$ shown in eq 3. The physical parameters used in the calculation are $\varepsilon_f = 7.08 \times 10^{-10}$ F/m, $\mu = 8.91 \times 10^{-4}$ Pa·S, $\mu_K = 7.616 \times 10^{-8}$ m^2/sV, $\mu_{Cl} = 7.909 \times 10^{-8}$ m^2/sV, and the double-stranded DNA radius $a = 1$ nm.

Acknowledgment. This research is supported partially by the Japan Society for the Promotion of Science (JSPS) through its "Funding Program for World-Leading Innovative R&D on Science and Technology".

Supporting Information Available: Discussions on controlling DNA transport through Al_2O_3 nanopores, effect of dragging force due to untranslocated parts in the *cis* chamber, and threshold voltages for DNA capturing. This material is available free of charge *via* the Internet at http://pubs.acs.org.

REFERENCES AND NOTES

1. Kasianowicz, J. J.; Brandin, E.; Branton, D.; Deamer, D. W. Characterization of Individual Polynucleotide Molecules Using a Membrane Channel. *Proc. Natl. Acad. Sci. U.S.A.* **1996**, *93*, 13770–13773.
2. Meller, A.; Nivon, L.; Brandin, E.; Golovchenko, J.; Branton, D. Rapid Nanopore Discrimination between Single Polynucleotide Molecules. *Proc. Natl. Acad. Sci. U.S.A.* **2000**, *97*, 1079–1084.
3. Dekker, C. Solid-State Nanopores. *Nat. Nanotechnol.* **2007**, *2*, 209–215.
4. Branton, D.; Deamer, D. W.; Marziali, A.; Bayley, H.; Benner, S. A.; Butler, T.; Di Ventra, M.; Garaj, S.; Hibbs, A.; Huang, X.; *et al.* The Potential and Challenges of Nanopore Sequencing. *Nat. Biotechnol.* **2008**, *26*, 1146–1153.
5. Zwolak, M.; Di Ventra, M. Colloquium: Physical Approaches to DNA Sequencing and Detection. *Rev. Mod. Phys.* **2008**, *80*, 141–165.
6. Kang, X.; Gu, L.-Q.; Cheley, S.; Bayley, H. Single Protein Pores Containing Molecular Adapters at High Temperatures. *Angew. Chem., Int. Ed.* **2005**, *117*, 1519–1523.
7. Akeson, M.; Branton, D.; Kasianowicz, J. J.; Brandin, E.; Deamer, D. W. Microsecond Time-Scale Discrimination Among Polycytidylic Acid, Polyadenylic Acid, and Polyuridylic Acid as Homopolymers or as Segments within Single RNA Molecules. *Biophys. J.* **1999**, *77*, 3227–3233.
8. Meller, A.; Nivon, L.; Branton, D. Voltage-Driven DNA Translocations through a Nanopore. *Phys. Rev. Lett.* **2001**, *86*, 3435–3438.
9. Zwolak, M.; Di Ventra, M. Electronic Signature of DNA Nucleotides *via* Transverse Transport. *Nano Lett.* **2005**, *5*, 421–424.
10. Lagerqvist, J.; Zwolak, M.; Di Ventra, M. Fast DNA Sequencing *via* Transverse Electronic Transport. *Nano Lett.* **2006**, *6*, 779–782.
11. Tsutsui, M.; Taniguchi, M.; Yokota, K.; Kawai, T. Identifying Single Nucleotides by Tunnelling Current. *Nat. Nanotechnol.* **2010**, *5*, 286–290.
12. Huang, S.; He, J.; Chang, S.; Zhang, P.; Liang, F.; Li, S.; Tuchband, M.; Fuhrmann, A.; Ros, R.; Lindsay, S. Identifying Single Bases in a DNA Oligomer with Electron Tunnelling. *Nat. Nanotechnol.* **2010**, *5*, 868–873.
13. Muthukumar, M. Mechanism of DNA Transport through Pores. *Annu. Rev. Biophys. Biomed.* **2007**, *36*, 435–450.
14. Li, J.; Talaga, D. S. The Distribution of DNA Translocation Times in Solid-State Nanopores. *J. Phys.: Condens. Matter* **2010**, *22*, 454129.
15. Fologea, D.; Uplinger, J.; Thomas, B.; McNabb, D. S.; Li, J. Slowing DNA Translocation in a Solid-State Nanopore. *Nano Lett.* **2005**, *5*, 1734–1737.
16. Ghosal, S. Effect of Salt Concentration on the Electrophoretic Speed of a Polyelectrolyte through a Nanopore. *Phys. Rev. Lett.* **2007**, *98*, 238104.
17. Trepagnier, E. H.; Radenovic, A.; Sivak, D.; Geissler, P.; Liphardt, J. Controlling DNA Capture and Propagation through Artificial Nanopores. *Nano Lett.* **2007**, *7*, 2824–2830.
18. Keyser, U. F.; Koeleman, B. N.; van Dorp, S.; Ralph M. M. Smeets, D. K.; Lemay, S. G.; Dekker, N. H.; Dekker, C. Direct Force Measurements on DNA in a Solid-State Nanopore. *Nat. Phys.* **2006**, *2*, 473–477.
19. He, H.; Scheicher, R. H.; Pandey, R.; Rocha, A. R.; Sanvito, S.; Grigoriev, A.; Ahuja, R.; Karna, S. P. Functionalized Nanopore-Embedded Electrodes for Rapid DNA Sequencing. *J. Phys. Chem. C* **2008**, *112*, 3456–3459.
20. Nam, S.-W.; Rooks, M. J.; Kim, K.-B.; Rossnagel, S. M. Ionic Field Effect Transistors with Sub-10 nm Multiple Nanopores. *Nano Lett.* **2009**, *9*, 2044–2048.
21. Nam, S.-W.; Lee, M.-H.; Lee, S.-H.; Lee, D.-J.; Rossnagel, S. M.; Kim, K.-B. Sub-10-nm Nanochannels by Self-Sealing and Self-Limiting Atomic Layer Deposition. *Nano Lett.* **2010**, *10*, 3324–3329.
22. Wong, C. T. A.; Muthukumar, M. Polymer Capture by Electro-osmotic Flow of Oppositely Charged Nanopores. *J. Chem. Phys.* **2007**, *126*, 164903.

23. Muthukumar, M. Theory of Capture Rate in Polymer Translocation. *J. Chem. Phys.* **2010**, *132*, 195101.
24. Storm, A. J.; Storm, C.; Chen, J.; Zandbergen, H.; Joanny, J.-F.; Dekker, C. Fast DNA Translocation through a Solid-State Nanopore. *Nano Lett.* **2005**, *5*, 1193–1197.
25. Smeets, R. M. M.; Keyser, U. F.; Krapf, D.; Wu, M.-Y.; Dekker, N. H.; Dekker, C. Salt Dependence of Ion Transport and DNA Translocation through Solid-State Nanopores. *Nano Lett.* **2006**, *6*, 89–95.
26. Behrens, S. H.; Grier, D. G. The Charge of Glass and Silica Surfaces. *J. Chem. Phys.* **2001**, *115*, 6716–6721.
27. Stein, D.; Kruithof, M.; Dekker, C. Surface-Charge-Governed Ion Transport in Nanofluidic Channels. *Phys. Rev. Lett.* **2004**, *93*, 035901.
28. van Dorp, S.; Keyser, U. F.; Dekker, N. H.; Dekker, C.; Lemay, S. G. Origin of the Electrophoretic Force on DNA in Solid-State Nanopores. *Nat. Phys.* **2009**, *5*, 347–351.
29. Manning, G. S. The Molecular Theory of Polyelectrolyte Solutions with Applications to the Electrostatic Properties of Polynucleotides. *Q. Rev. Biophys.* **1978**, *11*, 179–246.
30. Chang, H.; Kosari, F.; G., A.; Alam, M. A.; Vasmatzis, G.; Bashir, R. DNA-Mediated Fluctuations in Ionic Current through Silicon Oxide Nanopore Channels. *Nano Lett.* **2004**, *4*, 1551–1556.
31. Kowalczyk, S. W.; Tuijtel, M. W.; Donkers, S. P.; Dekker, C. Unraveling Single-Stranded DNA in a Solid-State Nanopore. *Nano Lett.* **2010**, *10*, 1414–1420.
32. Skinner, G. M.; van den Hout, M.; Broekmans, O.; Dekker, C. D. N. H. Distinguishing Single- and Double-Stranded Nucleic Acid Molecules Using Solid-State Nanopores. *Nano Lett.* **2009**, *9*, 2953–2960.
33. Chen, P.; Mitsui, T.; Farmer, D. B.; Golovchenko, J.; Gordon, R. G.; Branton, D. Atomic Layer Deposition to Fine-Tune the Surface Properties and Diameters of Fabricated Nanopores. *Nano Lett.* **2004**, *4*, 1333–1337.
34. Venkatesan, B. M.; Dorvel, B.; Yemenicioglu, S.; Watkins, N.; Petrov, I.; Bashir, R. Highly Sensitive, Mechanically Stable Nanopore Sensors for DNA Analysis. *Adv. Mater.* **2009**, *21*, 2771.
35. Venkatesan, B. M.; Shah, A. B.; Zuo, J.-M.; Bashir, R. DNA Sensing Using Nanocrystalline Surface-Enhanced Al_2O_3 Nanopore Sensors. *Adv. Funct. Mater.* **2010**, *20*, 1266–1275.
36. Mirsaidov, U.; Comer, J.; Dimitrov, V.; Aksimentiev, A.; Timp, G. Slowing the Translocation of Double-Stranded DNA Using a Nanopore Smaller Than the Double Helix. *Nanotechnology* **2010**, *21*, 395501.
37. Deamer, D. W.; Branton, D. Characterization of Nucleic Acids by Nanopore Analysis. *Acc. Chem. Res.* **2002**, *35*, 817–825.
38. Ai, Y.; Liu, J.; Zhang, B.; Qian, S. Field Effect Regulation of DNA Translocation through a Nanopore. *Anal. Chem.* **2010**, *82*, 8217–8225.